Part II

Project Summaries

Applied Mathematics

Time-Domain Algorithms for Computational Electromagnetics

Bradley Alpert
Leslie Greengard (New York University)
Thomas Hagstrom (University of New Mexico)

Acoustic and electromagnetic waves, including radiation and scattering phenomena, are increasingly modeled using time-domain computational methods, due to their flexibility in handling wide-band signals, material inhomogeneities, and nonlinearities. For many applications, particularly those arising at NIST, the accuracy of the computed models is essential. Existing methods, however, typically permit only limited control over accuracy; high accuracy generally cannot be achieved for reasonable computational cost.

Applications that require modeling of electromagnetic (and acoustic) wave propagation are extremely broad, ranging over device design, for antennas and waveguides, microcircuits and transducers, and low-observable aircraft; nondestructive testing, for turbines, jet engines, and railroad wheels; and imaging, in geophysics, medicine, and target identification. At NIST, applications include the modeling of antennas (including those on integrated circuits), waveguides (microwave, photonic, and at intermediate terahertz frequencies), transducers, and in nondestructive testing.

The objective of this project is to advance the state of the art in electromagnetic computations by eliminating three existing weaknesses with time-domain algorithms for computational electromagnetics to yield: (1) accurate nonreflecting boundary conditions (that reduce an infinite physical domain to a finite computational domain), (2) suitable geometric representation of scattering objects, and (3) high-order convergent, stable spatial and temporal discretizations for realistic scatterer geometries. The project is developing software to verify the accuracy of new algorithms and reporting these developments in publications and at professional conferences.

Local Nonreflecting Boundary Conditions. A problem that has been revisited this year is that of nonreflecting boundary conditions for the wave equation (and Maxwell's equations). Although earlier work of these researchers was successful in producing a procedure that is both spectrally accurate and highly efficient, its lack of flexibility in the shape of the boundary limits the variety of settings in which it has been adopted. Alpert and his collaborators have since attempted to generalize the nonreflecting boundary procedures to rectangular domains. This year they became convinced that the highly nonlocal dependencies inherent in nonreflecting boundary conditions can be circumvented (or localized) by looking somewhat inside the domain. This hypothesis, arising in part by analytical work by Warchall, has prompted a renewed attempt to formulate an exact local nonreflecting boundary treatment. This work continues.

Impact. A paper presenting recent NIST collaborative research appeared: "Near-Field, Spherical-Scanning Antenna Measurements with Nonideal Probe Locations," R. C. Wittmann, B. K. Alpert, and M. H. Francis, *IEEE Transactions on Antennas and Propagation* **52** (8) (2004), pp. 2184-2186. A paper on an inner product for scattering problems, "Half Space Representation of Acoustic Waves from Compact Sources," B. Alpert and Y. Chen, has been accepted for publication in *Communications in Pure and Applied Mathematics*. The work has been recognized by researchers developing methods for computational electromagnetics (CEM) and has influenced work on these problems at Boeing and HRL (formerly Hughes Research Laboratories). It has also influenced researchers at Yale University and University of Illinois. In each of these cases, new research in time-domain CEM is exploiting discoveries of the project.

This work has been supported in part by the Defense Advanced Research Projects Agency (DARPA).

Resonant Optical Scattering by Nanoscale Periodic Structures

Andrew Dienstfrey

The emerging ability of scientists to fabricate materials at nanometer length scales has created new possibilities for the engineering of materials with novel optical scattering properties. These devices will have tremendous impact in a variety of commercial, defense-related, and scientific applications: magneto-optic storage, micro-antenna arrays, integrated optical circuits, quantum computing hardware, to name a few. Essential for the successful development of these devices, are specialized computational tools which can accurately guide researchers in fabrication and modeling efforts.

Broadly speaking, these materials are composite, nanoscale dielectric and metallic scatterers arranged in a periodic manner so as to harness resonant phenomena in their interaction with electromagnetic fields. Instances go by various names depending on the scientific community and/or the desired objective of the research. Research into *photonic crystals* is yielding new techniques for the use of patterned dielectric structures as nanoscale optical waveguides. In the emerging field of *plasmonics*, electromagnetic fields are coupled to surface electron fields in metals. The resulting interactions allow, for example, for highly-collimated optical beam formation. Control of this process could have significant impact in the development of future magneto-optic storage devices. Finally, research in *meta-materials* includes new ways of modeling frequency-selective services. These surfaces reflect or transmit light at variable yet controlled frequencies with high-efficiency and selectivity. They are currently the subject of intense study by multiple groups within NIST's Electromagnetics Division (EEEL) as well as in the physics community at large. In addition to having applications as tunable optical pass-band filters, these structures present theoretical modeling challenges as several homogenization theories that are currently in use entail paradoxical effects concerning the refraction and propagation speeds of electromagnetic fields.

As an entry point into this field, MCSD research over the past year has focused on developing a suite of programs for precise simulation of scattering of electromagnetic waves by meta-material structures. The computational task is challenging in that the problem requires full vector solutions to Maxwell's Equations capable of simultaneously capturing both near and far-fields so as to bridge, respectively, the coupling of resonances dictated by nanometer scale structures to the macroscopic scales at which fields become accessible to homogenization theories. In brief, the program represents near-fields as truncated expansions of spherical multipole vector fields. Although these vector functions appear in the classical solution to *single* sphere scattering initiated by Mie in 1903, algorithms for translating expansions, which are required in the case of scattering by *multiple* spheres, are still under development today. Given the complicated nature of these functions, efficient representations are essential and the program leverages several years of research efforts undertaken by Ron Wittmann and other NIST scientists working in near-field antenna measurements. With these choices made, there is an additional mathematical complication in that the model postulates an *infinite* array of scatterers. Therefore, it is necessary to develop algorithms for computing certain doubly-infinite formal sums. The convergence properties of these sums are extremely subtle and constitute a mathematical hurdle that must be overcome. Finally, the interplay between length scales associated with individual small scatterers on the one hand, and on the other hand an effective large scatterer consisting of infinitely many individuals, requires computations to go deep into what are referred to as evanescent modes so as to achieve numerical convergence. The instabilities associated with these modes are legion. The program overcomes these problems through careful scalings of internal representations. All of these problems have been addressed and initial results are promising. It is anticipated that, in parallel to fabrication and measurement experiments also underway within NIST, the computational tools developed by MCSD will aid in testing these theories.

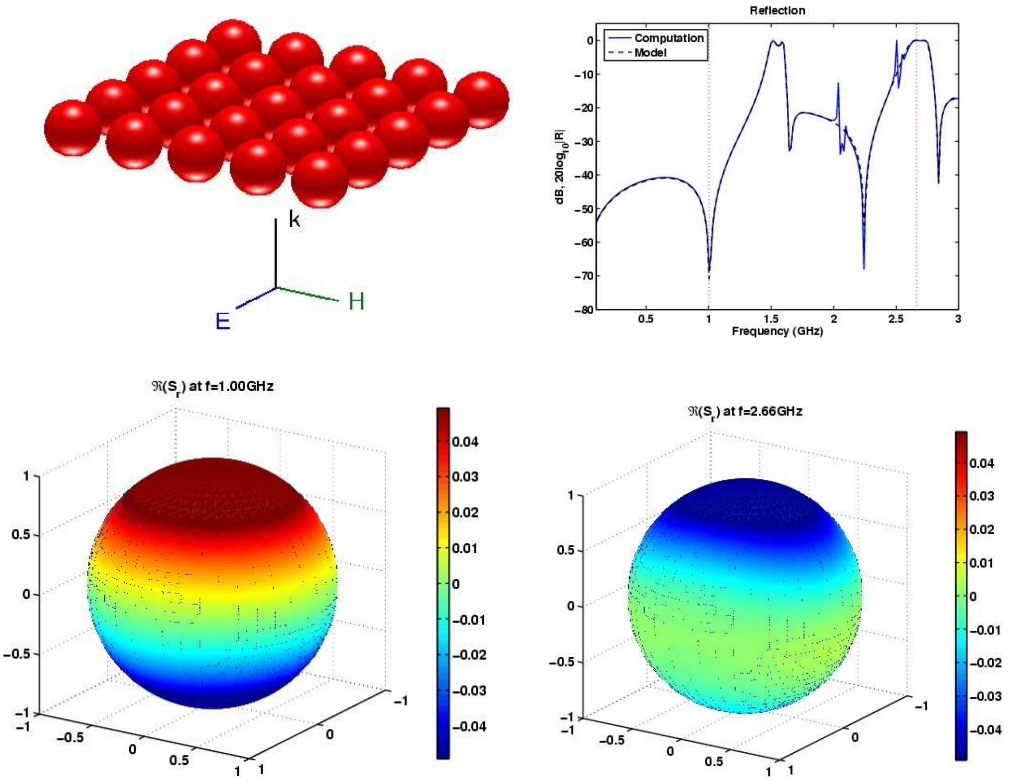

Results of computation of electromagnetic scattering by a proposed meta-film. The upper left shows the geometry of the scatterers. The spheres are composed of yttrium iron garnet (YIG) and exhibit high dielectric and magnetic susceptibilities relative to free space ε=15, μ=45). The sphere radii and lattice constant are r=5 mm, d=12.79 mm respectively. In the computation the array extends to infinity. The upper right shows the magnitude of the reflection coefficients predicted by a NIST model and determined by the computation. Note the deep minimum in reflected energy predicted by both model and computation at $f \cong 1$ GHz and again at $f \cong 2.25$ GHz. The lower plots show the radial component of the electromagnetic energy flux at the surface of each scatterer. The plot on the left is consistent with the energy flow induced by the incident planewave radiation. Of theoretical interest is the inverted energy flow through the sphere at the frequency of maximum reflection shown in the lower right.

The plots above show results of a computation a meta-film consisting of an infinite array of dielectric/paramagnetic spherical scatterers situated in the XY-plane, illuminated from below by a linearly-polarized planewave traveling upward in the z-direction. This structure is being fabricated at microwave scales and measured in a waveguide by members of Magnetics and Radio-Frequency Electronics Groups (EEEL). In addition, a model has been developed by members of the Radio-Frequency Fields Group. The subplot in the upper left shows the geometry of the scatterers. In the upper right the magnitudes of the reflection coefficients predicted by the model and the computation are plotted as functions of frequency. One observes good agreement between the model and computation. In particular, both predict the deep minimum in reflection at 1GHz which implies a particularly high transmission of electromagnetic energy at this frequency. However, the computation predicts other resonances (for example, the structure near 2GHz) that the model can not account for at present. The nature of these resonances is currently under investigation.

Finally, the computation allows for the resolution of energy flow at unprecedented scales. The two lower plots show the magnitudes of the radial component of electromagnetic energy flux at the surface the spherical scatterers at two different frequencies. The plot on the left shows the flux at

the frequency of maximum transmission (approximately 1GHz). The negative values at the bottom and positive values at the top of the sphere (blue and red, respectively) are consistent with the incident planewave penetrating into the sphere at the bottom and emerging through the top with little impedance. The subplot on the lower right is in stark contrast. At this frequency (approximately 2.7GHz) the spheres exhibit maximum reflection, minimum transmission. Here one observes a reversal of energy flow from the previous picture in that, at least on the surface of the sphere, the energy is entering the sphere from the top and exiting from the bottom. This reversed flow of energy lies at the heart of the paradoxes and disputes circulating in the physics community studying meta-material structures. It is hoped that in the coming year continued investigation with the set of computational tools developed by MCSD will aid in resolution of some of these problems.

Phase-Field Modeling of Solidification under Stress

Geoffrey B. McFadden
Julia Slutsker (NIST MSEL)
James A. Warren (NIST MSEL)
A. L. Roytburd (U. of Maryland)
Peter W. Voorhees (Northwestern U.)
K. Thornton (U. of Michigan)

Melting and solidification into either a crystalline or amorphous state in nano-volumes are basic mechanisms of modern phase change recording. This process exploits an amorphous-to-crystalline phase change to record information onto electronic media such as DVDs. Due to the density difference between phases, transformations in confined volumes are accompanied by internal stresses. Thus, it is necessary to take into account the effect of internal stress during phase change recording. In this project we have modeled this "writing" process by considering melting and solidification in a confined volume.

To simulate melting/solidification we employ a phase field model. Phase-field modeling is an effective approach for the analysis and prediction of the evolution of complex microstructures during phase transformations. This approach has been particularly successful when it has been applied to solidification problems. For single-component system the standard phase-field method requires solving two equations: the time dependent Ginsburg-Landau phase-field equation and the equation of heat transfer. The phase field model that we develop includes stress field during non-isothermal solidification of a one-component system. These stresses can be external or internal, i.e. they can arise as a result of boundary conditions at the external surface or they can be a result of elastic interactions between the phases. Thus, the phase field model takes into account the simultaneous evolution of three fields: a phase field, a temperature field and a stress/strain field.

To demonstrate this approach we consider the solidification and melting of a confined sphere. For this simple system the complete numerical solutions taking into account the time-space evolution of temperature, order parameter and strain-stress field is obtained. The simulation shows that at some boundary and initial conditions the evolution of a spherical symmetry system results in steady states corresponding time-independent distribution of order-parameter and uniform temperature. Comparison results of phase field modeling and thermodynamic analysis of a sharp-interface model shows that these steady states are equilibria which exist in systems with fixed volume. The analysis of these equilibrium states allows us to estimate the value of interface energy that are then verified by a phase field calculation of the energy of plane liquid/solid interface. The model can be used to simulate the process of "writing" to electronic media that exploit an amorphous-to-crystalline phase change for recording information.

Part of this work represents a collaboration with researchers at Northwestern University under an NSF Nanoscale Interdisciplinary Research Team (NIRT) grant. K. Thornton spent four weeks visiting MCSD under this program, and G. McFadden visited Northwestern and presented results at a nanotechnology workshop at Northwestern that was funded through the grant.

A conference proceedings paper on this work has been published: J. Slutsker, A. L. Roytburd, G. B. McFadden, and J. A. Warren, "Phase Field Modeling of Solidification and Melting of a Confined Nano-particle," International Workshop on Nanomechanics, July 14-17, 2004, Pacific Grove, CA, Tze-jer Chuang and Peter Anderson, eds.

This work has been supported in part by the National Science Foundation (NSF).

Lateral Deformation of Diffusion Couples

G. McFadden
W. Boettinger (NIST MSEL)
S. Coriell (NIST MSEL)
J. Warren (NIST MSEL)
R. F. Sekerka (Carnegie Mellon U.)

The recent interest in the design and operation of nanoscale systems has prompted increased attention to problems of stress and diffusion in thin layers and other small-scale geometries. The underlying process represents a complicated modeling problem in which the diffusion process is affected by the deformation due to plastic and elastic forces in the sample, and, conversely, the deformation field is affected by interdiffusion that may induce strain due to differences in the molar volumes of the various constituents. This inherent coupling makes an understanding of the process challenging, and progress is often possible only through a combination of modeling, analysis, and computations.

In this project G. McFadden collaborated with W.J. Boettinger, S.R. Coriell, and J.A. Warren of the Metallurgy Division, MSEL, and R.F. Sekerka, of Carnegie Mellon University on the modeling of stress effects during interdiffusion of solute in a diffusion couple. The work involves a continuum model that describes the creation and annihilation of lattice vacancies at defects in the crystal, which can produce swelling or shrinkage of the sample locally.

The Kirkendall effect is a well-known consequence of a disparity in the intrinsic diffusion coefficients of the components in alloy diffusion couples. The effect has three manifestations: a shift of inert markers parallel to the diffusion direction (deformation with pure axial displacement), lateral shape changes (displacements with a component orthogonal to the diffusion direction), and the formation of voids. We have developed a model that includes a description of the uniaxial Kirkendall effect, capturing the deformation parallel to the diffusion direction, and at the same time obtaining the concomitant lateral deformation. A solution to the coupled equations describing diffusion and deformation can be obtained using Fourier analysis for the case under consideration. We obtain limiting behavior for thin and thick cylinders and slabs, and compute numerical results of the model for the lateral shape change which compare favorably with experimental measurments of the deformation observed in gold-silver alloys. This work has been submitted for publication in *Acta Materialia*.

An extension of the work is being used to model the bending of a thin plate, for which experimental data is also available. This work is intended to address problems in which stress is produced in nano-scale samples due to the effects of multicomponent diffusion.

The Effect of Contact Lines on the Rayleigh Instability of a Crystalline Interface

G. McFadden
K. Gurski (George Washington U.)
M. Miksis (Northwestern U.)

In continuum models of nanoscale structures, the importance of surface energy effects often become a critical factor as the ratio of surface to volume increases. In previous work the effects of surface tension anisotropy on interfacial instabilities in crystalline rods or wires was considered. These instabilities can lead to break-up of the structures, with associated mechanical or electrical failure of the system. These instabilities are generalizations of the classical modes studied by Lord Rayleigh in liquid jets, and are capillary effects that reflect the lower surface energy associated with the decrease in surface area near a necking region.

We are currently generalizing our previous work for isolated crystalline bodies by including the effects of a substrate that supports the crystalline rod or wire. The junction of the rod and substrate at a contact line can significantly stabilize the system, since the contact line restricts the form of perturbations that can lower the overall energy of the system. We have performed an energy analysis of the system that leads to a coupled eigenvaue problem, with associated boundary conditions arising from the balance of energies at the contact line. The results are relevant for studies of quantum wires on circuit boards or other types of substrates.

This work represents a collaboration with researchers at Northwestern University under an NSF Nanoscale Interdisciplinary Research Team (NIRT) grant.

This work has been supported in part by the National Science Foundation (NSF).

Configurational Forces at a Liquid-Liquid Interface

G. McFadden
D. Anderson (George Mason U.)
M Gurtin (Carnegie Mellon U.)
E. Fried (Washington U.)
P. Cermelli (U. of Torino, Italy)

The motion of two fluid phases and the interface separating them has been a problem of scientific and industrial interest for centuries. Applications in which the understanding of the interface between two fluid phases is critical continue to emerge. As the complexity of these problems increases, particularly the complexity of the physics occuring at the interface, there is an increased need for robust methods for identifying the appropriate interfacial conditions to be applied in continuum models of the fluid--fluid interface. Equilibrium interfacial conditions for phase-transforming systems have been successfully derived based on variational arguments. However, these fail to extend to nonequilibrium settings where dissipative effects such as fluid viscosity are important.

In this work we address the problem of formulating directly nonequilibrium interfacial conditions for an interface between two fluids. The approach we adopt here is based on the formalism of configurational forces as developed by Gurtin. We specifically apply these ideas to fluid-fluid systems in which phase transitions may occur. Of particular interest are interfacial conditions such as the nonequilibrium version of the Gibbs-Thomson equation. Our discussion of configurational forces leads naturally to the inclusion of effects such as interfacial viscosity and interface kinetics. This work is being submitted to the *Journal of Fluid Mechanics*.

Phase-Field Model of Line Energies at a Corner or Tri-Junction

G. McFadden
A. Wheeler (U. of Southampton)

Phase-field models of multiphase systems represent interfaces between different thermodynamic phases as regions of finite width, rather than mathematically-sharp surfaces. These models can incorporate physical effects such as interface kinetics and surface tension anisotropy in a natural manner, since the underlying formalism is based on a consistent thermodynamic description of the system. If the level of surface tension anisotropy is large enough, the interface can develop corners where the system prefers to omit certain high-energy orientations all together. Surprisingly, phase-field models can describe such missing orientations even though the interface has finite width; to do so, the solutions develop singularities through the whole interfacial region, where each contour of the phase-field variable describing the interface has a corner with limiting angles that are determined by the surface tension anisotropy. It is natural to associate a line energy with such a corner, and to consider further generalizations of the phase-field formalism that selectively smooth the corners at an even smaller length scale. To do this, we have developed a model in which the free energy of the system consists of both convectional gradient energy terms that account for the surface energy, and a new term that involves the square of the Laplacian to account for line energies. We performed an asymptotic analysis that recovers the conventional sharp corner conditions in the limit of small smoothing. Professor Wheeler visited for two one-week periods this year during this collaboration.

Linear Stability of Cylindrical Couette Flow in the Convection Regime

G. McFadden
M. Ali (King Saud U., Riyadh, Saudi Arabia)

The viscous fluid flow created between differentially rotating coaxial cylinders has provided a fertile testing ground for both linear and nonlinear stability theory. Beginning with the work of G.I. Taylor in 1923, numerous experimental and theoretical studies on flow transitions and morphologies of supercritical circular Couette flow have appeared. Initial studies on thermally-driven circular Couette flow were motivated by technological problems in the cooling of rotating electrical machinery. Early theoretical attacks neglected gravity and usually considered only axisymmetric disturbances in the limit of infinite aspect ratio. There has been a renewed interest in the problem of radially heated rotating flows, partially from a continued effort to enhance the cooling of rotating machinery, but also with the aim of understanding and controlling instabilities in nematic liquid crystal systems, in chemical vapor deposition processes, and in the solidification of pure metal.

The stability of viscous isothermal circular-Couette flow generated by rotation of the inner cylinder is controlled by the radius ratio, the aspect ratio, and the Taylor number. Stationary counter-rotating toroidal cells of uniform width stacked one above the other appears at a critical Taylor number. In the absence of rotation, natural convection between vertical differentially heated concentric cylinders depends crucially on the magnitude of the imposed thermal heating and the system aspect ratio. Early experimental studies fostered the identification of three distinct flow regimes in both planar and cylindrical gaps: conduction, transition, and convection. Here we consider the convection regime, where axial boundary layers form along each cylinder walls, and a vertical temperature gradient develops in the interior of the sample. We have developed an analytical solution for the base flow in the convection regime in a vertical annulus with a rotating inner cylinder and a stationary outer cylinder. The stability of this base flow is then computed numerically with respect to both axisymmetric and asymmetric disturbances. A paper has been submitted to *Physics of Fluids*.

Linear Stability of Spiral Poiseuille Flow with a Radial Temperature Gradient

D. L. Cotrell
G. B. McFadden

For fluid flow in an annulus driven by the combination of an axial pressure gradient, rotation of the inner and outer cylinders, and a radial temperature gradient (spiral Poiseuille flow with a radial temperature gradient), we are investigating the transition from the simplest flow possible (steady flow with two nonzero velocity components and a radial temperature gradient that vary only with radius) to the next simplest flow possible (steady flow with three nonzero velocity components and a temperature profile that vary in the radial and axial directions). This work is motivated by electrochemical processes in rotating cylinder electrodes, heat transfer in rotating machinery, flow-amplified electrophoretic separations, and vortex flow reactors for shear-sensitive biological systems. This work extends the case of isothermal spiral Poiseuille flow for which D. Cotrell and A. Pearlstein (University of Illinois at Urbana-Champaign) recently computed complete linear stability boundaries for several values of the radius ratio and rotation rate ratio, and shows how the centrifugally-driven instability (beginning with steady or azimuthally-traveling-wave bifurcation of circular Couette flow) connects to a non-axisymmetric Tollmien-Schlichting-like instability of nonrotating annular Poiseuille flow (flow driven solely by an axial pressure gradient). Results for the non-isothermal case show that the stability boundary shifts either up or down depending on the sign of the temperature difference. For the isothermal case, it is also known that in many instances there is no instability for small enough axial flow rates. For the non-isothermal case, however, we have shown that for any nonzero temperature difference between the inner and outer radii, a new non-isothermal mode of instability causes the base state to be destabilized under these conditions. This work has been submitted to *Physics of Fluids* for publication.

Axial Flow Effects on the Linear Stability of Circular Couette Flow with Viscous Heating

D. L. Cotrell
G. B. McFadden

For fluid flow in an annulus driven by the combination of an axial pressure gradient and rotation of the inner and outer cylinders, G. McFadden and D. Cotrell are investigating the effect axial flow has on the linear stability of circular Couette flow with viscous heating. We note that it is extremely important to consider viscous heating in hydrodynamic stability calculations and experiments, because unlike externally imposed temperature gradients, viscous heating is a strong function of the fluid properties and cannot be easily controlled or eliminated. The analysis extends previous results with no axial flow (and computes the correct asymptotic behavior at large temperatures, a case for which we believe incorrect results are in the literature), and accounts for non-axisymmetric disturbances of infinitesimal amplitude. D. Cotrell has implemented the linear stability analysis for this case using spectral methods, but because the number of collocation points needed to fully resolve the strong internal thermal layer is large, He has also solved the linear stability problem by solving a two point boundary value problem (using the program Support) whose results will be used to check solutions in parts of parameter space for which the spectral method approach requires significant spatial resolution. Comparison between the two methods is good, but limited due to the fact that the boundary value problem approach uses Newton iteration to find critical eigenvalues and the domain of convergence is very small. Because of this, Cotrell has implemented spectral domain

decomposition in the spectral collocation code. Because this generates a global matrix eigenvalue system that is sparse, Cotrell is in the process of implementing the sparse eigenvalue solver ARPACK which finds only a specified number of eigenvalues clustered around a point you pick (i.e., the real part of the temporal growth rate is zero).

Linear Stability of Modified Couette Flow

D. L. Cotrell
G. B. McFadden

The stability of flow in the annular region between two concentric cylinders driven by rotation of either one or both cylinder walls has been investigated since the work of Taylor (1923). One of the simplest geometric perturbations of the "standard" flow is when one of the axisymmetric boundaries is allowed to have an axially-periodic radius. This problem is important is wavelength selection, cases where one might want to prescribe the wavelength of the resulting vortices, and in trying to stabilize axisymmetric Taylor vortices beyond the range seen for the smooth walled case. D. Cotrell has used the finite element method to implement the axisymmetric linear stability for this steady 2-D base state, and is currently in the process of using previous computational and experimental results to validate the code. Cotrell is in the process of implementing the nonaxisymmetric case as well.

Materials Data and Metrology for Applications to Machining Processes, Frangible Ammunition, and Body Armor

Timothy Burns
Stephen Banovic (NIST MSEL)
Richard Fields (NIST MSEL)
Michael Kennedy (NIST MEL)
Li Ma (NIST MSEL)
Lyle Levine (NIST MSEL)
Steven Mates (NIST MSEL)
Richard Rhorer (NIST MEL)
Eric Whitenton (NIST MEL)
Howard Yoon (NIST PL)

The usefulness of computer simulations of rapid deformation processes using commercial finite-element software packages is often limited by the lack of material response data in the regimes of interest. For example, high-speed machining processes involve the plastic deformation of materials at very high rates of deformation, and this leads to rapid heating of the material in the cutting zone. The relationship of stress (force per unit area) to strain (a dimensionless tensor quantity that measures how much a material deforms in compression and shear), often referred to as the material constitutive response (or the stress-strain curve in simple cases), can be much different at high strain rates and high temperatures than typical "handbook" data. Therefore, a vital step in the development and implementation of effective machining models is to provide appropriate stress-strain relationships for materials of interest to industry. In 2001, a project was started at NIST, *Materials Data and Metrology for Machining Simulation*, which included building a unique testing apparatus that couples a traditional Kolsky (split-Hopkinson) high-strain-rate material response testing bar, with an existing NIST fast pulse-heating facility. The Kolsky compression test involves sandwiching a sample of the test material between two long, hardened steel rods. One of the steel rods is impacted by a shorter rod of the same material, sending a stress pulse into the sample. While the steel rods remain elastic in their response to the impact loading, the sample deforms plastically at a rapid rate of strain, and instrumentation on each of the long steel rods can be used to determine the stress-strain response of the test material. The goal of the new facility has been to develop the capability to preheat a material sample rapidly using an electrical pulse, and then almost immediately perform a Kolsky bar

compression test, thereby providing high-strain-rate, pulse-heated material response data that would be useful for high-speed machining studies. While the pulse-heating and temperature control capabilities were being developed for the Kolsky bar, and experiments were being performed on materials of interest in the automobile and aircraft industries, the twin towers at the World Trade Center in New York City were destroyed, and several NIST laboratories were tasked by Congress with analyzing the specific sequence of events that led to the collapse of the buildings. Constitutive response data were required for the many types of steel that had been used in constructing the towers, and the NIST Kolsky Bar Facility was employed for this purpose. When ATP funding for the original project ended in FY2004, all of the major goals had been met, and a unique materials testing laboratory had been built with the help of personnel from several NIST laboratories, along with the help of interested personnel from universities and other government laboratories with expertise in the many different areas required to get the facility up and running.

During the past fiscal year, while studies have continued on the modeling of high-speed machining of materials of interest in manufacturing, funding has been obtained from the National Institute of Justice (NIJ) through the NIST Office of Law Enforcement Standards (OLES) to use the NIST Kolsky Bar to study the constitutive response of frangible bullets (i.e., ammunition made from materials other than lead that breaks up on impact), and to develop a related tension-testing bar to study the mechanical behavior of soft body armor woven from fibers of the advanced polymeric materials PBO (Zylon) and Aramid (Kevlar). The test data will be used by the US Department of Justice to determine what actions are required to ensure that soft body armor provides adequate protection to police officers in the field. Experimentally validated finite element models of bullet-vest interactions will be developed as part of this new program, which is expected to be funded for another two fiscal years.

This work has been supported in part by the NIST Advanced Technology Program (ATP) and the National Institute of Justice (NIJ).

Micromagnetic Modeling

Michael Donahue
Donald Porter
Robert McMichael (NIST MSEL)
Eduardo Martinez (U. of Salamanca)

http://math.nist.gov/oommf/

Advances in magnetic devices such as recording heads, field sensors, magnetic nonvolatile memory (MRAM), and magnetic logic devices are dependent on an understanding of magnetization processes in magnetic materials at the nanometer level. Micromagnetics, a mathematical model used to simulate magnetic behavior, is needed to interpret measurements at this scale. MCSD is working with industrial and academic partners, as well as with colleagues in the NIST MSEL, PL, and EEEL, to improve the state-of-the-art in micromagnetic modeling.

Michael Donahue and Donald Porter in MCSD have developed a widely used public domain computer code for doing computational micromagnetics, the Object-Oriented Micromagnetic Modeling Framework (OOMMF). OOMMF serves as an open, well-documented environment in which algorithms can be evaluated on benchmark problems. OOMMF also provides a fully functional micromagnetic modeling system, handling both two and three-dimensional problems, with sophisticated extensible input and output mechanisms. OOMMF has become an invaluable tool in the magnetics research community. In fiscal year 2004 alone, the software was downloaded more than 2,400 times, and use of OOMMF was acknowledged in more than 40 peer-reviewed journal articles.

OOMMF is part of a larger activity, the Micromagnetic Modeling Activity Group (muMAG), formed in 1995 to address fundamental issues in micromagnetic modeling through two activities: the development of public domain reference software, and the definition and dissemination of standard problems for testing modeling software. MCSD staff members are involved in development of the standard problem suite as well. There are currently four standard problems in the suite, testing both static and dynamic magnetization properties. Two additional standard problems are in development, dealing with modeling of thermal effects and dealing with model artifacts due to discretization of material boundaries.

In large devices, random thermal effects tend to be self-canceling, but as device size decreases thermal effects grow in relevance. This is especially true in high sensitivity low field magnetic sensors, where performance is generally limited by thermal noise. A four-laboratory NIST Competence project (EEEL, MSEL, PL and ITL) to design a new generation of such sensors is in progress, and proper modeling of thermal effects within OOMMF is a key objective. Eduardo Martinez, a visiting summer student from University of Salamanca, provided insight into the established traditions of thermal modeling.

The MCSD micromagnetic project produced six journal papers and three conference presentations in the fiscal year 2004. Project staff also contributed to the National Nanotechnology Initiative Interagency Workshop on Instrumentation and Metrology for Nanotechnology.

This work is supported in part by the NIST Competence Program.

Optimization Problems in Smart Machining Systems

David E. Gilsinn
Florian Potra
Laurent Deshayes (NIST, MEL)
Alkan Donmez (NIST, MEL)
Robert Ivester (NIST, MEL)
Richard Rhorer (NIST, MEL)
Lawrence Welsch (NIST, MEL)
Eric Whtenton (NIST, MEL)

The goals of Smart Machining Systems (SMS) are to produce the first and every product correct, improve the response of the production system to changes in demands (just in time), realize rapid manufacturing, and provide data on an as needed basis. These systems are envisioned to have the capability of: self recognition and communication of their capabilities to other parts of the manufacturing enterprise; self monitoring and optimizing their operations; self assessing the quality of their own work; and self learning and performance improvement over time. To accomplish this, the SMS must cope with uncertainties associated with models and data. Robust optimization is an approach for coping with such uncertainties.

Optimization plays a crucial role in SMS. A general optimization problem consists in determining some decision variables $x_1, x_2, \ldots, x_n$, such as feed, depth of cut, spindle speed, in such a way that a set of given constraints are satisfied and a desired objective function is optimized. The constraints are determined by both empirical, heuristics and theoretical considerations, and they can usually be expressed as a system of inequalities. If we denote by x the vector of decision variables and by $f_0(x)$ the objective function, then the optimization problem can be written as

$$\text{minimize} \quad f_0(x) \tag{1}$$

$$\text{subject to} \quad f_i(x) \le 0, \qquad i = 1, 2, \ldots, m. \tag{2}$$

An example of an objective function that we would like to minimize in machining is the surface location error. The above general form of an optimization problem can handle also objective functions that we would like to maximize, like the material removal rate. This is accomplished by

replacing $f_0(x)$ with $-f_0(x)$ in (1). If the objective function $f_0(x)$, as well as the functions $f_1(x), f_2(x), \ldots, f_m(x)$ defining the constraints, such as cutting force, machine tool power and torque, tool life, surface roughness and spindle speed, are linear in the decision variables, then the optimization problem (1)-(2) becomes a linear programming problem (LP) that has been extensively studied, and for which efficient algorithms are known. However, in most application both the objective function and the functions defining the constraints are nonlinear. By introducing an additional variable x_0, we can always consider that the objective function is linear. Indeed it is easily seen that that the optimization problem (1)-(2) is equivalent to

$$\text{minimize} \quad x_0 \tag{3}$$

$$\text{subject to} \quad f_0(x) - x_0 \le 0, \tag{4}$$

$$f_i(x) \le 0, \quad i = 1, 2, \ldots, m. \tag{5}$$

While in a traditional deterministic setting, where $f_0(x), f_1(x), \ldots, f_m(x)$ are considered precisely determined, the form (3)-(5) can be conveniently extended to deal with uncertainty in the data defining the optimization problem. Indeed, in real applications the functions $f_0(x), f_1(x), \ldots, f_m(x)$ depend on some parameters $\varsigma_1, \varsigma_2, \ldots, \varsigma_p$ that are only approximately known. In some cases we can define an "uncertainty set", or set of possible parameter values, $U \subset R^p$ that contain all possible values of the parameter vector ς. If U contains a single vector then we are in the traditional deterministic setting. Otherwise, we consider the robust optimization problem

$$\text{minimize} \quad x_0 \tag{6}$$

$$\text{subject to} \quad f_0(x, \varsigma) - x_0 \le 0, \quad \forall \varsigma \in U \tag{7}$$

$$f_i(x, \varsigma) \le 0, \ i = 1, 2, \ldots, m, \ \forall \varsigma \in U \tag{8}$$

The robust optimization problem above aims at determining the vector of decision variables x such that the objective function is minimized and the constraints are satisfied *for all* possible values of the parameter vector ς. Although this seems hopeless, recent progress in optimization theory and practice shows that for many engineering problems we can formulate robust optimization problems that can be efficiently solved by modern optimization algorithms.

Currently a model for maximizing the material removal rate for a turning center by estimating the appropriate tool feed rate and turning speed has been proposed by MEL. It currently requires only an LP solver, but a script has been written in Matlab to examine the effect of varying parameters over a wide range of values. Graphs of feasible regions have been developed that can aid a machine operator in selecting the optimal or near-optimal parameter settings. The current script has been interfaced to GUI by MEL so that an operator can test the consequences of selecting parameters within the allowed ranges. A full robust optimization code requires the development of a more extensive script, but the current version allows MEL Engineers to begin studying the affects of parameter adjustment on material removal rate and comparing results against machining experiments.

Hierarchical Control of Systems Governed by Differential Equations

Anthony Kearsley
Paul Boggs (Sandia National Laboratories)
Jon Tolle (University of North Carolina)

The study of optimal control problems arising in the control of fluids in non-standard geometries has become an extremely active area of research. Motivated by a desire to detect, simulate and even control contaminant transport (perhaps from security applications) numerical algorithms are actively being investigated by numerous research groups. Our small group has developed a theory and approach to these problems based on multiple but ranked (or hierarchical) objectives. Typically, one wants to control a state equation, an approach involving well-ordered multiple objectives. These problems belong to the class of problems called multicriteria optimization. There is no unique mathematical formulation of these types of problems. In practice these problems are often solved by minimizing a weighted sum of the deviations from the targets with the weights corresponding to the preferences. Another formulation, sometimes referred to as goal programming, insists that the preferred targets must be satisfied to within certain tolerances and the others are reduced as much as possible within these constraints. Both of these approaches involve the choice of a set of weights or tolerances for which there can be little theoretical guidance. Yet another approach, called bilevel optimization nests optimization problems, optimizing with respect to one target and using the solutions as parameters in a larger problem.

We have successfully developed a nonlinear programming approach to these hierarchical optimization problems. Given a fairly arbitrary (general) geometry, a constitutive flow equation and a collection of well-ordered objectives, we have derived an optimality system whose solution yields optimal controls and state variables that seek to achieve objectives in the order that they have been placed.

Analysis of Extrema Arising in Laser Sampling Techniques

Anthony Kearsley
Peter Ketcham
Geoffrey McFadden

Raman spectroscopy is a technique that measures molecular vibrational energies of chemical compounds. It is a form of vibrational spectroscopy complementary to infrared absorption. Raman spectra are generated by a monochromatic light source (e.g., a laser) to a sample and detecting the light that is inelastically back-scattered. The majority of the scattered light has the same energy as the laser; this is elastic scattering or Rayleigh scattered radiation. A very small portion of the incident laser light (~10-6%) is scattered inelastically by a discrete amount of energy that is related to the molecular vibrational energy of the molecular bond. This is known as Raman scattering (see Figure), which can be used to help elucidate the structural characteristics of the sample.

Raman spectroscopy instruments offer the capability to rapidly screen an unknown sample without requiring the operator to physically handle or prepare the sample. Additionally, Raman can be performed through a variety of container types, including glass, paper, and some plastics. These characteristics make Raman a suitable candidate for field analyses of a forensic nature. An evaluation of several portable Raman instruments was undertaken to help identify requirements for an improved fieldable Raman instrument that could be used by first responders. Key characteristics of these systems include portability, energy control, and ease of use by field agents who may not have extensive training in spectroscopy.

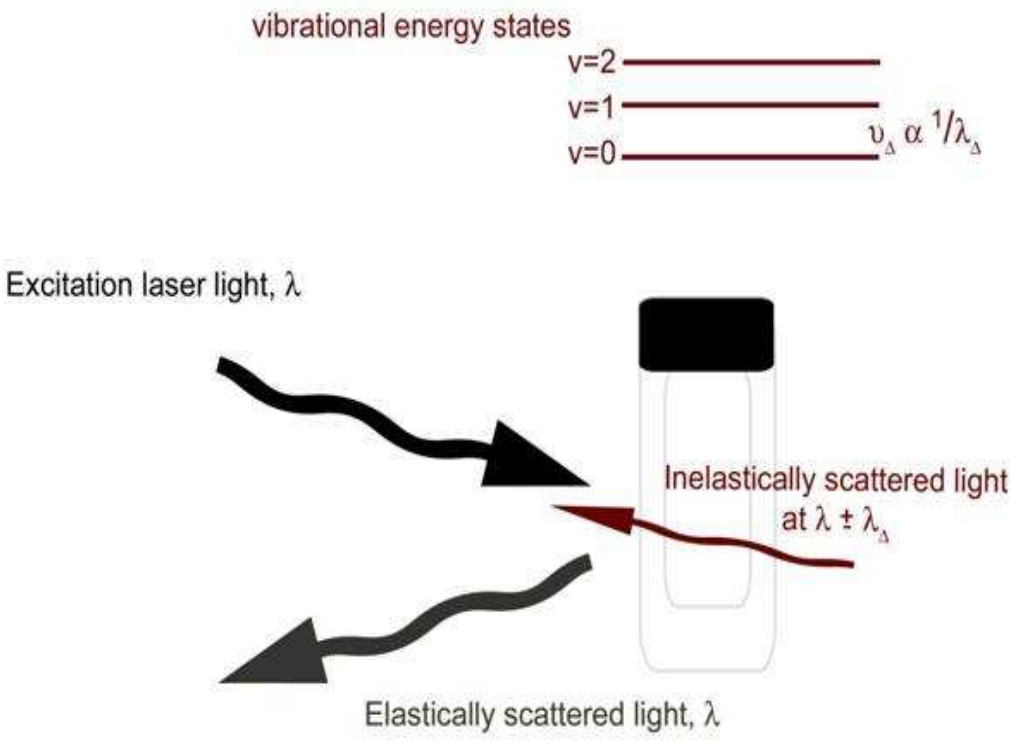

An illustration of the Raman scattering process.

To determine specifications for the next-generation field-portable Raman systems each of the instruments is in the process of being evaluated for use by first responders in the field. During the course of these evaluations, the need for an improved, fully automated, sample identification and peak-matching algorithm became clear. The algorithm currently under development consists of multi-stage computer processing that

1. selects peaks and troughs in spectroscopic data in a fully automated fashion,
2. identifies a sub-selection of statistically relevant peaks,
3. compares the statistically relevant peaks to a previously compiled database of spectral files, and
4. calculates a score that indicates the strength of the correlation between the collected spectrum and a database entry.

We have started developing an algorithm that we believe may be appropriate for this application. The real strength of this algorithm is that it functions independent of the number of data points, data-point spacing, spectral range, and the instrument's resolving power. This is intended to forestall the need for additional database development each time instrument specifications or optical designs are changed.

This work is partially supported by the Federal Bureau of Investigation (FBI).

Automated Numerical Algorithms for Advanced Mass Spectrometry and Standard Reference Materials

Javier Bernal
Anthony Kearsley
Peter Ketcham
Charles Guttman (NIST MSEL)
William Wallace (NIST MSEL

Modern mass spectrometry (MSpec) has been producing important material science information in a wide variety of scientific applications. Most recently, this work has become very important in the analysis and identification of chemicals for pharmaceutical industries, homeland security applications and manufacturing optimization. Loosely speaking a mass spectrometer (see Figure 1) detects the presence of chemicals inside a sample by bombarding the sample, suspended in a matrix, with ions (in the form of a laser) and then counting the ions "bounce" off the matrix prepared sample (see Figure 2). Each chemical causes ions to bounce off in a different way thus leaving a signature. Very often, one is interested in testing for the presence of a particular chemical inside a sample material, a MSpec experiment can be designed to result in large peaks being produced when the chemical in question is detected by ions (for example one must identify, separate and sum the matrix peaks present in the Bradykinin MSpec output in Figure 3). This accurate method for determining the presence of chemicals has been employed with more and more frequency by scientists.

While very detailed chemical procedures have been developed for MSpec sample preparation, very little work has been done on the development of automated numerical methods for the analysis of MSpec output. Today, analysis of such data requires a huge investment of time by highly trained professionals, limiting its usefulness in law enforcement and homeland security applications.

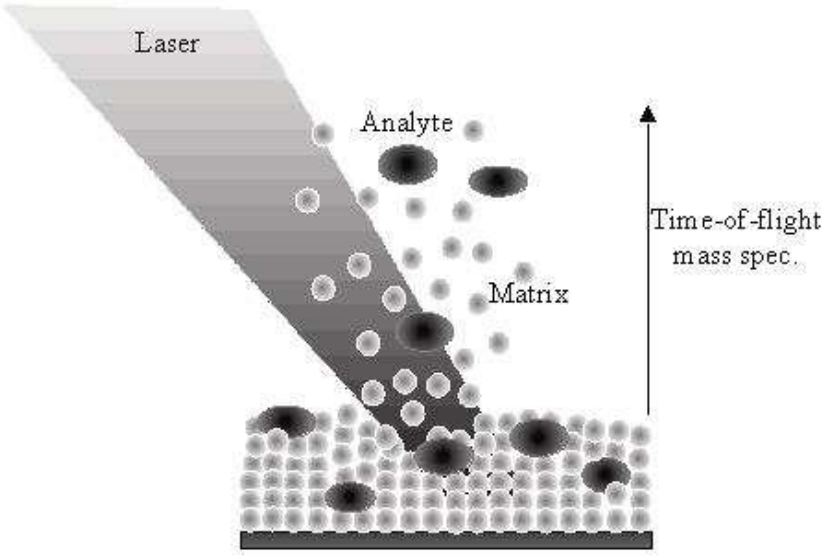

Figure 1: Illustration of MALDI Time-of-Flight Mass Spectrometer

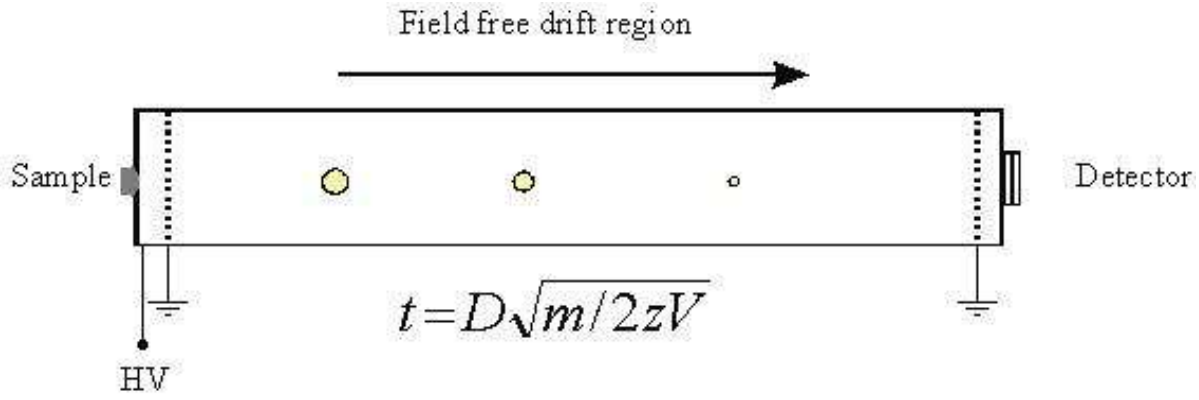

Figure 2: Detection mechanism in MALDI Time-of-Flight Mass Spectrometer

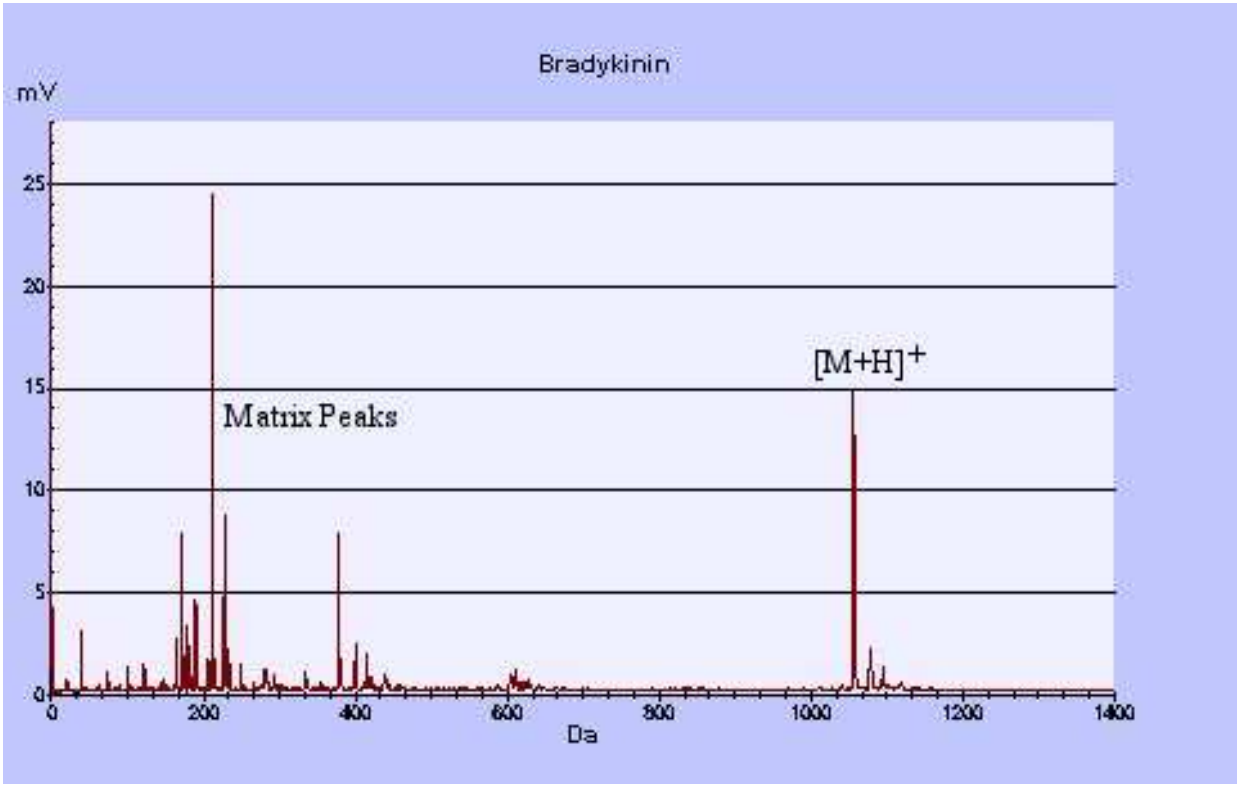

Figure 3: Bradykinin Mspec Output

The objective of this project is to develop a reliable, and robust algorithm for *automatically* analyzing raw output from mass spectrometers and to demonstrate the algorithm by building a from-everywhere accessible public-domain web-based tool making a high quality implementation of the algorithm available. An elementary version of the algorithm has been made available on the web and has been very popular (the algorithm was accessed by over 5,000 different sites in its first month of availability). This trial web tool was constructed in such a way that one can directly analyze noisy mass spectrometer output and generate unbiased machine-independent analysis of the noisy data in a timely fashion, greatly reducing (or eliminating) the need for laborious and painstaking manual analysis.

Modern mass spectrometers produce astonishingly high-quality data. Scientists are regularly faced with the difficult and time consuming task of sorting through many enormous noisy data sets in search of data structures (for example one must assume a “peak” shape or a “trough” shape) corresponding to the presence of chemical in question. Likewise, to determine the similarity or origin of fibers requires the analysis of chemical compositions usually acquired with a mass spectrometer. Because of unavoidable measurement errors committed when using a mass spectrometer outputs from different laboratories, machines or test runs can vary even when analyzing identical samples. When this data is then analyzed to determine the presence of a chemical substance that professionals must carefully examine the data by hand to identify the structure indicative of the chemical presence in question. This expensive and time consuming task is usually done with the aid of packaged computational algorithms many of which are `black-box' codes sold by software vendors or by companies manufacturing mass spectrometer hardware. In practice, these codes are often massaged into performing correctly by changing large numbers of algorithmic input parameters and/or testing subsets of the output data independently before analyzing the entire mass spectrometer output. Numerical behavior of currently available software can vary drastically as a function of numerous extraneous factors including parameter selection, choice of peak shape for example, machine precision, and even the computer platform on which the software is being run. Simply put, this is a very difficult problem.

We have succeeded in developing, implementing and testing an algorithm that, given raw MSpec data, can efficiently identify peak and trough structure without assuming any a priori size or shape structure. This algorithm is unique in that it requires no arbitrary parameter selection but instead allows the user to input a readily available estimate of machine noise produced by all time of flight mass spectrometers. Preliminary results are promising as the algorithm is now being used to analyze MSpec data (by members of the Polymer division at NIST, staff members at the Bureau of Alcohol Tabbacco and Firearms, the Federal Bureau of Investigation, the National Institutes of Health and a number of private companies).The webtool has been mentioned in general science journals like *Science*, *Nature* and *Radiochemistry News*.

The following papers related to this project have recently appeared.

- Bernal, C. Guttman, A. Kearsley and W. Wallace ``Automated Peak Picking and Integration Algorithm for Mass Spectral Data'', in Proceedings of the 51st ASMS Conference on Mass Spectrometry and Allied Topics, June 2003, Montreal Canada.
- J. Bernal, C. Guttman, A. Kearsley and W. Wallace ``A Numerical Method for Mass Spectral Data Analysis'', Applied Mathematics Letters (in revision)
- W. Wallace, A. Kearsley C. Guttman ``An Operator-Independent Approach to Mass Spectral Peak Identification and Integration'', Analytical Chemistry, 76, 2446-2452 (2004).

Mathematical Problems in Construction Metrology

Javier Bernal
David Gilsinn
Christoph Witzgall
Geraldine Cheok (NIST, BFRL)
Alan Lytle (NIST, BFRL)
William Stone (NIST, BFRL)

During the past decade, laser-scanning technology has developed into a major vehicle for wide-ranging applications such as cartography, bathymetry, urban planning, object detection, and dredge volume determination, just to name a few. The NIST Building and Fire Research Laboratory is actively investigating the use of such technology for monitoring construction sites. Here laser scans taken from several vantage points are used to construct a surface model representing a particular scene. Another aspect of the project envisions that CAD-generated geometry sets will be transformed into a library of 3D construction site objects, which will serve multiple purposes during construction. The objects would be loaded into an augmented simulation system that tracks both equipment and resources based on real-time data from the construction site obtained from laser scans. With some additional enhancements, the end result will be a world model of the site, in which as-built conditions can be assessed, current construction processes can be viewed as they occur, planned sequences of processes can be tested, and object information can be retrieved on demand. A project could be viewed and managed remotely using this tool. Pick-and-place control of construction site objects is another application of the 3D construction site object library. With automation and robotics entering on construction site scene, vision systems, such as LADAR (laser direction and ranging), will be incorporated for real time object identification, using the 3D library templates. Once objects, such as I-beams, are located and their pose determined, robotic crane grippers can be manipulated to acquire the I-beam.

LADAR technology is currently being tested by the NIST Building and Fire Research Laboratory for locating equipment on construction sites. LADAR scans of I-beams of multiple lengths and angular poses relative to the scanning LADAR have been generated (See Figure 1). A database of design specifications for potential I-beam candidates has been created. The LADAR scans generate a large number of points, ranging in the millions, in a typical scan that can be acquired in a matter of seconds. These scans usually contain a large number of noisy data values arising from ground hits to phantom pixels caused by beam splitting at sharp edges.

Figure 2 shows the scan obtained by the LADAR. Although each of the points in the figure are associated with an (x, y, z) coordinate relative to the LADAR, the identification of the nature of the objects scanned is not as clear as a photograph provides. Whereas the photograph provides a clear image it does not provide coordinate information. The challenge then is to use the database of design specifications, in this case of I-beams, to locate an object in the scanned image that essentially matches the length, width and height of an I-beam from the database and to report its center-of-mass location and angular pose relative to the LADAR. The scanned image consist of nothing more than coordinate points. In order to compare efficiency as well as speed, two algorithms have been developed to process the coordinate points obtained from a scan. One algorithm depends on binning of the scanned points to reduce the number of points processed. The bins are then examined to identify those that are likely to be phantom points or floor hits. These bins are eliminated from further analysis. Bins are then grouped into potential objects and bounding boxes place around them. These boxes are compared with bounding boxes defining the I-beams in the database and the best fit one is reported as the likely I-beam in the scan. At the same time to center and pose of the object bounding box is reported. The second algorithm relies on using Triangulated Irregular Networks (TINs) to mesh the scanned data. The density of the triangulated points is then examined to identify those triangle groups most likely to form solid objects in the scanned field-of-view. The bounding box procedure is then applied to these groups and the bounding boxes are compared with the bounding boxes of I-beams specified in the database. Again, location and pose relative to the LADAR is also determined.

Joining cent-of-mass estimates with principle components analysis has been shown to be a reliable method of determining location and pose of the I-beams.

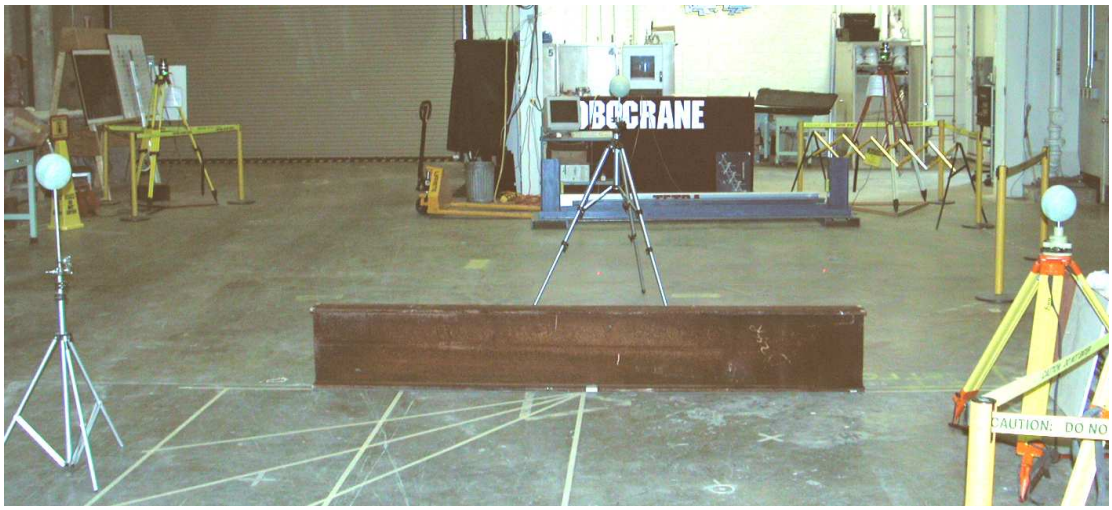

Figure 1: This figure shows the experimental configuration used for scanning an I-beam by a LADAR placed approximately at the camera location. The white lines on the floor are alignment marks for setting the I-beam at different angles relative to the LADAR. The spheres on tripods are located for coordinate registration with a world coordinate system.

Figure 3 shows a comparison being made between a bounding box of an I-beam from the database and a potential object in the field-of-view of the scanner. The red outlined box is the bounding box constructed from the database and the blue outlined box is the bounding box of the scanned object. Note that the algorithms have isolated the potential objects from the noise, floor hits and phantom pixels. Figure 4 shows a close fit between an I-beam bounding box constructed from the database and an isolated object scanned by the LADAR.

Other approaches to modeling objects in 3D construction sites have also been investigated including multivariate splines and finite elements. Traditional least squares fitting can lead to ringing at sharp edges of objects or buildings. A new minimum energy principle has been developed that fits Clough-Tocher finite elements to objects with sharp edges in such a way that ringing is suppressed. The minimization algorithm joins a Gauss-Seidel relaxation algorithm with a reweighting and regularization algorithm. It has shown promise on various test problems but requires further analysis to understand the nature of the algorithms convergence.

Urban environments provide challenges for first responders. Situation management for them now finds it desirable for the command and control center to have instant access to the location of both threats and assets. That is, they need to know the 3D whereabouts of their personnel during an incident. To date, no such system exists that will reliably and accurately track the movement of emergency and law enforcement personnel inside a building. Previous substantial research by NIST BFRL has proven that ultra-wideband tracking is viable through several meters of non-metallic construction material. Crucial to the accuracy of the use of ultra-wideband tracking is knowledge of the quantitative behavior of electromagnetic (EM) wave propagation through construction materials, since EM propagation speed varies dramatically depending on the type of material involved (e.g. concrete, brick, masonry block, plywood, etc.). Lack of accurate material properties could yield location estimates that are in error by a factor of 10 or more from their true location.

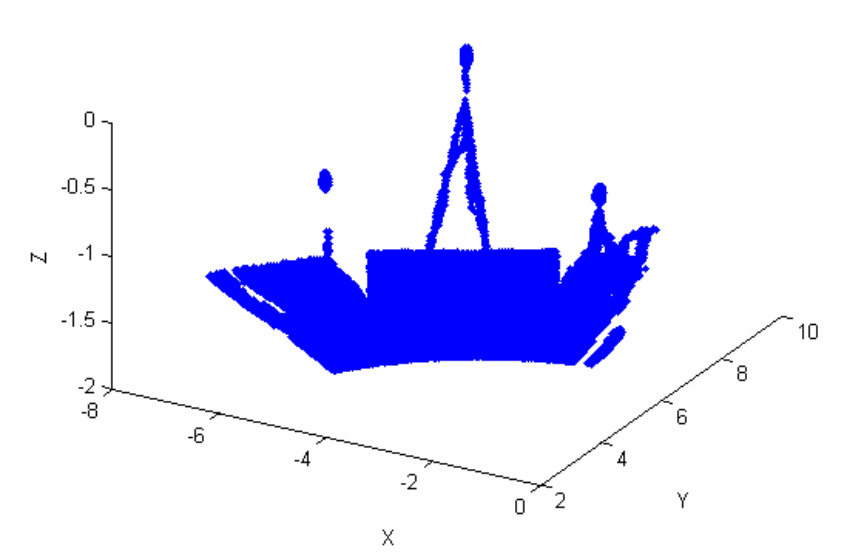

Figure 2: This figure shows the results of a LADAR scan of the I-beam in Figure 1. The flat areas on either side of what appears to be the I-beam are floor hits. Notice the results of hits on the three tripods.

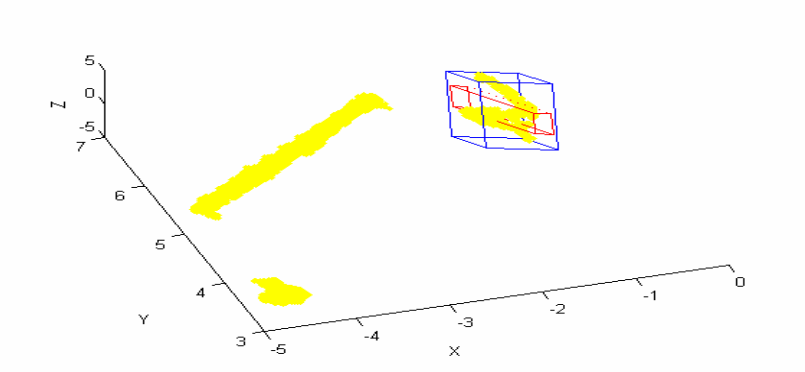

Figure 3: This figure shows the lack of fit between a bounding box defining an ideal I-beam (red) from the database and a bounding box defining an object in the LADAR field-of-view (blue).

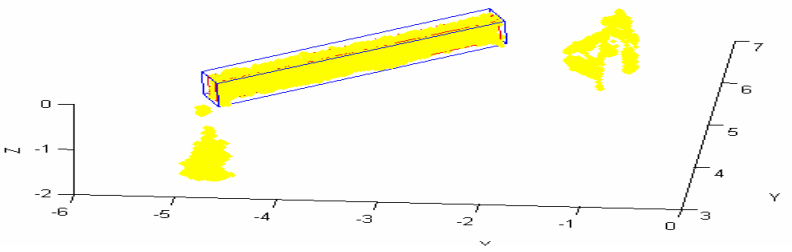

Figure 4: This figure shows the close fit of a bounding box defining an ideal I-beam (red) and a bounding box defining the isolated scanned object (blue).

The key characteristic needed to predict 3D location is the frequency-dependent dielectric constant for a broad class of construction materials. NIST BFRL began investigating ultra-wideband methods for tracking the movement of objects inside buildings as early as 1994. That program initially investigated time-of-flight through-wall tracking in the 0.5 to 2 GHz regime (which includes that of most cell phones) and then later extended the research to include all frequencies between 0.5 to 8 GHz.

BFRL obtained FY04 funds from the NIST Office of Law Enforcement Standards to investigate the possibility of computing the dielectric constants of construction materials. D. Gilsinn of MCSD was approached by BFRL to determine the feasibility of using this data and a known model from the EM literature that related dielectric constants to the transmission coefficients available in the experimental data, as a way to estimate the dielectric constants of the materials. A script was written in Matlab to perform a nonlinear least squares estimate of the dielectric constants. For low frequency values in the 0.5 GHz range unique minima were obtained. However, as frequencies increase multiple minima showed up in the form of lobes. After consultation with colleagues in the EM field it became clear that the multiple minima were due to the fact that at higher frequencies it took multiple wavelengths to penetrate the material. For wavelengths approximately the width of the test material a single minimum was produced. Another thing that was found out was that the dielectric constants had to be treated as complex quantities. Thus it was necessary to search for minima in the complex plane. BFRL has proposed to OLES to continue the investigation of computing the dielectric constants in FY05.

This work was supported in part by the NIST Building and Fire Research Laboratory.

Modeling and Computational Techniques for Bioinformatics Based Data Mining

Fern Y. Hunt
Agnes O'Gallagher

The purpose of this project is to develop generic bioinformatics algorithms that can utilize large-scale and fast computational methods to perform the comparison and alignment of a large number of long biological sequences. Almost all methods currently in use are based on an optimization problem that is solved using the methods of dynamic programming. Starting from a Markov decision theory approach, we solve a linear programming problem. Our goal is to avoid the exponential increase in computation as the number of sequences increases and to avail ourselves of the high performance algorithms available for solving this type of problem. Potential applications for this work are in drug discovery where large numbers of sequence sites must be evaluated for use as drug targets and the development of of pharmacogenomic therapies, i.e. therapies that are tailored to genetic-makeup of the patient. Multiple sequence alignment also plays an important role in the characterization of biological threats.

The software package growing out of our algorithm development requires training data, i.e. a set of aligned sequences that are used to determine the underlying model parameters. Much of our time in 2004 was spent in looking for ways to obviate the need for this. For example rather than relying on data from sequences aligned by other methods we sought to construct data sequences by simulating (in a controlled way) the evolution of protein or DNA sequences.

We used the program ROSE to simulate the evolution of an entire bacterial genome. This produced a set of evolutionary related sequences that were used as a training set. Thus we were able to align the genomes of the original and several other sequences using our method. In addition to enhanced computational efficiency, the robustness to changes in the alignment due to changes in the input parameters can be measured. This is a feature that is to our knowledge, unique to our approach.

Last year we examined the sensitivity of the solutions of the linear programming problem to small changes in the costs. The latter could occur because of changes in the scoring matrix used to score the alignments. This year we examined the sensitivity of the alignments and found them to be quite robust. Theoretical calculations of the degree of sensitivity bear out our observations.

Three invited presentations including one hour talk at the American Mathematical Society were given. Two papers describing our work were submitted to refereed journals and both were accepted for publication.

Virtual Measurements from Computational Quantum Chemistry Models

Raghu Kacker
Karl Irikura (NIST CSTL)
Russell Johnson (NIST CSTL)

http://srdata.nist.gov/cccbdb

A virtual measurement is a prediction determined from a computational model together with its associated uncertainty for the value of a measurand. We are developing practical methods to quantify the uncertainty associated with the predictions from computational quantum chemistry models and also trying to address other important issues in quantum chemistry. Interest in virtual measurements is increasing for reasons of economics and safety. They are becoming critical in research and development of chemical processes, new materials, and drug discovery. Predictions from quantum chemistry models are usually reported without uncertainties making them incomplete and less useful. The uncertainties in computed values arise largely from systematic biases rather than random errors; therefore, a new approach is needed.

We have developed an approach to quantify the uncertainty associated with enthalpies of formation based upon the *Guide to the Expression of Uncertainty in Measurement*, published by the International Organization for Standardization (ISO) and the NIST Computational Chemistry Comparison and Benchmark Database (CCCBDB), which contains data for over 600 molecules, over 100 calculations for each molecule, and over 4000 vibrational frequencies (Irikura, K. K.; Johnson, R. D., III; Kacker, R. N. *Metrologia* **41** (2004), pp. 369-375). The challenging issue here is identifying a suitable class of molecules in the CCCBDB for which the biases are similar to the bias for the target molecule. Predictions from ab initio calculations of vibrational frequencies are scaled to compensate for their estimated differences from the experimental values. The scaling factors carry uncertainty, yet it is not quantified. We are in the process of quantifying these uncertainties. For the vibrational frequencies we found the uncertainties to be orders of magnitude larger than previously believed. We plan to continue extracting such information from the CCCBDB to determine the uncertainties for other calculated properties as well. By convention, uncertainties in quantum chemistry are expressed as intervals with a stated coverage probability such as 95 %. Often, the available information and the method of propagating uncertainties do not provide a definitive coverage probability. We are investigating the corresponding probability distributions. There is great interest in using quantum chemistry models to help identify unknown molecules by vibrational spectroscopy and to quantify the probability that the molecule is correctly identified.

Lipschitz Space Characterization of Images

Alfred S. Carasso

Previous MCSD work on characterizing the lack of smoothness of natural images, is gaining wide acceptance, and is influencing the direction of research in image analysis.

Most commonly occurring images *f(x,y)* display edges, localized sharp features, and other fine-scale details or *texture*. In particular, *f(x,y)* is very seldom a differentiable function at every point (x, y). Correct characterization of the lack of smoothness of images is a fundamental problem in image processing.

It turns out that so-called *Lipschitz spaces* are the appropriate framework for accomodating non-smooth images. The L^p Lipschitz exponent α for the given image, where $0 < \alpha < 1$, measures the fine-scale content of that image, provided the image is relatively noise free. Heavily textured imagery has low values for α, while large values of α indicate that the image is relatively smooth.

During the past year, four presentations of this general circle of ideas were made. The venues were the MCSD Colloquium, the University of Maryland Wavelet and Harmonic Analysis Seminar, the SIAM Image Science Conference in Salt Lake City, and the George Washington University Summer Program for Women in Mathematics. In addition, a MiniSymposium on *Loss and Recovery of Image Texture* was organized at the Salt Lake City SIAM Conference, featuring eight speakers and drawing a sizeable audience. A paper entitled "Singular Integrals, Image Smoothness, and the Recovery of Texture in Image Deblurring" was published in the *SIAM Journal on Applied Mathematics*, Volume **64**, Issue 5 (2004), pp. 1749-1774. That particular SIAP issue is notable for including four major papers on image analysis among its fourteen published articles, indicating strong current interest in this research topic.

Considerable effort was also expended in seeking U.S. Patent protection for MCSD's technique for measuring image Lipschitz exponents, and the accompanying new MCSD deblurring methodology. Intensive interaction with patent attorney Dr. Noreen Welch, of the Washington, DC law firm of Stevens, Davis, Miller and Mosher, over a three month period, resulted in the filing of an application entitled *Singular Integral Image Deblurring Method* on August 31 2004.

Improving Image Resolution in Nanotechnology

Alfred S. Carasso,
András E. Vladár (NIST MEL)

A recurring theme at the January 2004 *NIST Grand Challenge National Nanotechnology Workshop*, was the relatively low quality of current nanoscale electron microscopy micrographs, and the urgent need for improved imagery to support future research. Of major interest to the Nanoscale Metrology Group at NIST is the continuing development of improved mathematical tools for image analysis, and the use of such tools to effect measurable increases in resolution in state-of-the-art scanning electron microscopy. One very major difficulty lies in the large image sizes, often on the order of 1024x1024 pixels, or larger. This presents formidable computational challenges. Many new techniques are based on nonlinear partial differential equations, and typically require thousands of iterations, and several hours of CPU time, to achieve useful results. *Real-time* image processing algorithms are exceedingly rare and very highly sought after.

A fundamental problem in Scanning Electron Microscopy is the fact that the shape of the electron beam that produced the image is seldom known to the microscopist. Therefore, image deblurring must proceed without knowledge of the actual point spread function that caused the blur. Such so-called *blind deconvolution* is fraught with difficulty, and little authoritative discussion of this subject is to be found in most image processing textbooks.

Nevertheless, in recent years, considerable progress was achieved by MCSD in developing mathematical technologies that lead to real-time image processing algorithms. In addition, a unique new capability was created, the so-called *APEX method*, that can achieve useful blind deconvolution of 1024x1024 SEM imagery in about 60 seconds on current workstations. Because of its manifold applications, this technology is the subject of intense and continuing research and development.

Very recently, a new Hitachi Scanning Electron Microscope was acquired by the Nanoscale Metrology Group, capable of producing higher quality imagery than had previously been possible. A major challenge for MCSD's deconvolution algorithms was to demonstrate measurable increases in sharpening of such state of the art imagery. Two sharpness measures were used, the image Lipschitz exponent α, and the image discrete *total variation* or TV norm. Image sharpening increases the TV norm, due to the steepening of gradients, while it decreases the Lipschitz exponent as finer scale features become resolved. Examples of such sharpening are shown in Figures 1 and 2. In Figure 1A, the original 1024x1024 Tin sample micrograph has TV norm of 13000 and Lipschitz exponent $\alpha = 0.40$. The APEX-sharpened Figure 1B has TV norm = 34000 with $\alpha = 0.29$. In Figure 2A, the original 1024x1024 Magnetic Tape sample has TV norm = 14000 with $\alpha = 0.35$. The APEX-processed Figure 2B has TV norm = 39000 with α = 0.26. These very substantial sharpness increases are typical of those obtained in numerous other test images.

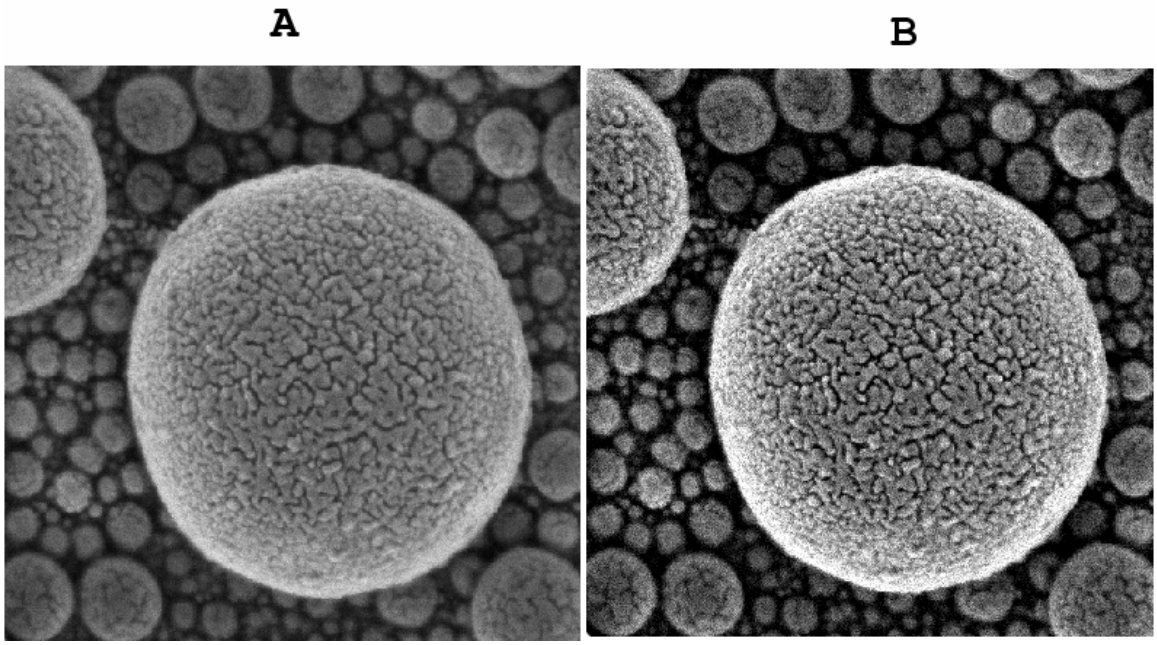

Figure 1. APEX blind deconvolution of state of the art Scanning Electron Microscope imagery produces measurable increases in sharpness. (A) Original 1024x1024 Tin sample micrograph has Lipschitz exponent $\alpha = 0.40$ and TV norm = 13000. (B) Sharpened image has $\alpha = 0.29$ and TV norm = 34000.

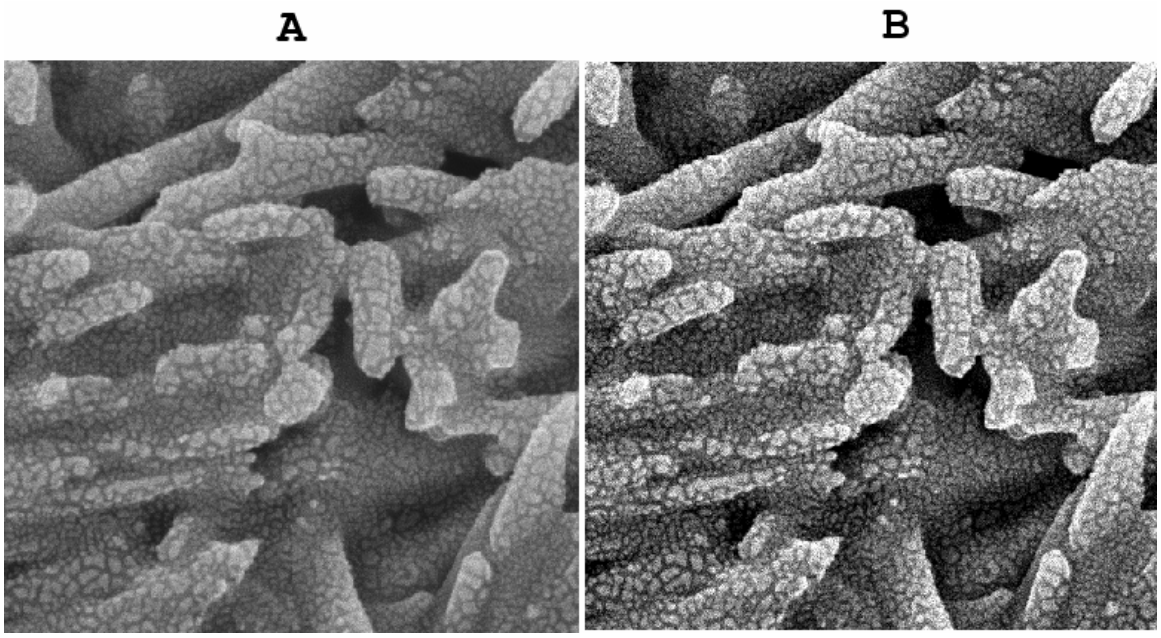

Figure 2. APEX sharpening of SEM imagery. (A) Original 1024x1024 Magnetic Tape sample has $\alpha = 0.35$ and TV norm = 14000. (B) Sharpened image has $\alpha = 0.26$ and TV norm = 39000.

Color Blind Deconvolution

Alfred S. Carasso

As previously observed, blind deconvolution of images is a difficult mathematical problem that is not fully understood, and one for which little reliable theoretical or computational expertise actually exists. MCSD's *APEX method*, as originally published in *SIAM Journal on Applied Mathematics* **63**, 2 (2002), pp. 593-618}, deals with gray-scale imagery. The method is based on identifying a blurring kernel in the form of a Lévy stable density function, by appropriate one dimensional Fourier analysis of the blurred image. Using that kernel, an ill-posed parabolic backwards in time continuation problem must then be solved to obtain the deblurred image.

Typically, the detected point spread function turns out to be too wide, *erroneously*. However, this can be compensated for by early termination of the continuation algorithm. This requires visual monitoring of the unfolding deconvolution process, by a user familiar with the physical or medical context underlying the image. Very striking results have been obtained with the APEX method, in quite diverse gray-scale imaging applications.

Blind deconvolution of color imagery appears to be a much harder problem. A color image can be decomposed into its RGB components, and the APEX method may be applied to each component in turn. However, the crucial APEX element that involves visual monitoring of the continuation algorithm is no longer feasible. An experienced user may be unable to decide whether or not the blue image, say, has been properly deblurred. Conceivably, in reconstituting the individual deblurred components into a single color image, one of the components may turn out to have been too aggressively sharpened, resulting in such false coloring as yellow eyes or green lips in Figure 3B. Clearly, considerable useful research remains be done, exploring various mathematical constraints that might be imposed to ensure proper balancing of the individual components. Most important, such constraints should avoid nonlinear formulations that require large numbers of iterations, as this would destroy the real-time advantage of the APEX method.

One real-time approach that has been found surprisingly successful is based on enforcing quasi conservation of radiant flux in each RGB component. In the above-mentioned backwards in time continuation problem, both the discrete L^1 and TV image norms can be calculated at each time step. Typically, the TV norm increases by a factor of 2 or 3, while the L^1 norm increases very slowly. It is found that useful color sharpening is obtained by terminating backwards continuation in each RGB component when the L^1 norm exceeds the original L^1 norm by more than 5%.

One intriguing potential application for color APEX processing lies in Hubble Telescope imagery. As shown in Figure 4, significant sharpening of some images appears to be possible.

Figure 3. Blind deconvolution of color imagery must result in correct balancing of RGB components and preserve natural coloring appropriate to subject matter. *Left:* Original Lizabeth Scott image. *Right:* Real time APEX sharpening with L^1 norm conservation preserves natural colors.

Figure 4. Hubble Telescope imagery presents interesting candidates for APEX processing. *Left:* Original Hubble image of Orion reflection nebula NGC 1999. *Right:* Real time APEX enhanced image.

Monte Carlo Methods for Combinatorial Counting Problems

Isabel Beichl
Francis Sullivan (IDA Center for Computing Sciences)

In the previous year we had developed a new method to estimate the number of independent sets in a graph. An independent set is a subset of the set of nodes of a graph where none of the subset has any connections with any other elements of the subset. This problem is important because of applications in thermodynamics and data communications. It is dual to the problem of counting the number of cliques in a graph and thus gives graph connectivity information. In this year, we applied the method to a first principles calculation of the hard sphere entropy constant in three dimensions. Calkin and Wilf had made an estimate in 2-dimensions. On the way to our 3-dimensional result, we reproduced their two-dimensional result. Calkin and Wilf also computed tight analytic upper and lower bounds on the constant. We have also been able to compute these bounds in three dimensions. This was done using the transfer matrix of the lattice, a technique originally developed in statistical mechanics. The trace of the transfer matrix for aperiodic lattices is just the largest eigenvalue of the transfer matrix for the periodic case. Calkin and Wilf didn't know this. Computing the largest eigenvalue can be done for these 0-1 matrices in very large cases by doing bit operations instead of using the floating point representation. Without this trick, we would not have been able to compute a large case and hence not obtain tight bounds.

Surface Reconstruction with the Power Crust

Javier Bernal

The problem of surface reconstruction is that of approximating the surface of an object from a set of sample points on the surface. Sample points are usually obtained from real objects with the aid of laser scanners.

The power crust is a piecewise-linear approximation of the surface of an object that is computed from an approximation of the medial axis of the object. The medial axis is a skeletal shape associated with the object with the property that each point in the medial axis is the center of a maximal empty ball that meets the surface of the object only tangentially at two or more points.

Currently a program is being implemented for computing the power crust. The main tools being used are the Voronoi diagram and the weighted Voronoi diagram or power diagram. The medial axis is first approximated by a subset of the Voronoi vertices of the set of sample points called poles. When the set of sample points is good the poles lie near the medial axis and the union of the Delaunay balls centered at poles inside the object approximates the object. The squared radii of the Delaunay balls centered at poles define weights on the poles and a power diagram of the set of weighted poles is computed. By taking advantage of the natural graph that the power diagram defines on the set of poles, poles are labeled as either inner or outer with respect to the object. The union of the power cells of inner poles is then a polyhedral solid that approximates the object and whose surface is the Power crust. Even when the set of sample points is not totally good because of noise or because it is too sparse, a good Power crust can usually be obtained by carefully selecting the poles.

Modeling the Behavior of Cryocoolers

Abbie O'Gallagher
John Gary

The REGEN3.2 package developed by John Gary and Abbie O'Gallagher over the last several years has become a dependable tool for researchers in cryocooler technology. It models the behavior of these devices and accepts a large number of parameters to describe the design, including the material properties of the device, the device geometry (screens, plates, spheres or some other configuration), its porosity, hydraulic diameter, cross sectional area, etc. It also has the capability of allowing a design that includes layers made up of different materials. Until now, Regen3.2 has not been capable of allowing those layers to have different configurations (for example screens in one layer and spheres in another) or different factors by which the thermal conductivity could be adjusted. This year A. O'Gallagher added these two capabilities.

Elastic Wave Model

Abbie O'Gallagher

Abbie O'Gallagher has been exercising a special version of a 3-D finite element wave code for Marv Hamstad of the Materials Reliability division. This work supports the database of waveforms that is being produced producing using this code. As part of this work, O'Gallagher revised a Matlab script for filtering output from the wave code. This work is reported in three papers appearing in the *Journal of Acoustic Emission.*:

- K. S. Downs, M. A. Hamstad and A. O'Gallagher, "Wavelet Transform Signal Processing to Distinguish Different Acoustic Emission Sources," *Journal of Acoustic Emission* **21** (2003), pp.52-69.
- M. A. Hamstad, K. S. Downs and A. O'Gallagher, "Practical Aspects of Acoustic Emission Source Location by a Wavelet Transform," *Journal of Acoustic Emission* **21** (2003), pp.70-94.
- M. A. Hamstad and A. O'Gallagher, "Modal-Based Identification of Acoustic Emission Sources in the Presence of Electronic Noise," to appear in *ournal. of Acoustic Emission*.

Measures of Approximation in Delay Differential Equations

David Gilsinn

Delay differential equations have arisen in the modeling of machine tool dynamics and, in particular, the problem of chatter. Machine tool chatter is a self-excited oscillation of a cutting tool against a machined workpiece. Acoustically it can be detected as a high frequency squeal in a machine shop. The suppression of chatter is significant to producing a high quality surface finish on the workpiece. Modeling chatter and other machining instabilities has been a problem of long-term interest to the NIST Manufacturing Engineering Laboratory. Mathematically, chatter is characterized as a limit cycle for a nonlinear delay differential equation.

D. Gilsinn of MCSD has implemented algorithms that compute various parameters needed in order to employ a precise measure of how near an approximate periodic solution is to the "real" limit cycle. The measure is more precise than a standard order-of-magnitude error estimate. Whereas in ordinary differential equations there are well-developed Green's function methods of determining the

initial conditions for periodic solutions as well as constructing fundamental solutions, in delay differential equations there are no such easily constructed relations. The stability of limit cycles is determined by the characteristic multipliers. For exact periodic solutions to delay equations there is always a characteristic multiplier of one with the location of the other characteristic multipliers identifying the nature of the stability of the solution. In ordinary differential equations the computation of characteristic multipliers becomes an algebraic problem. However, in delay differential equations the determination of characteristic multipliers can be performed by solving an eigenvalue problem for a Fredholm-type integral equation. Another parameter needed to implement the precise measure involves solving the adjoint delay differential equation associated with the variational equation of the nonlinear delay differential equation about the approximate solution. Solving the adjoint requires a reverse direction integration of the adjoint equation. However, delay differential equations usually solve in forward time steps. It is necessary then to formulate a variation of constants formula for the adjoint in such a way that only forward integration of the fundamental solution if required. Finally, a precise bound must be obtained relating the magnitude of a nonhomogeneous term to a solution in the case of a linear nonhomogeneous delay differential equation. Matlab programs have been written to compute these parameters and a precise location of the solution to a Van der Pol equation with delay has been demonstrated. Further study of more efficient algorithms for computing the necessary parameters is currently under way along with an analysis of the convergence of the parameter identification algorithms.

Modeling a Radioactive Decay Chain

Bert W. Rust
Dianne P. O'Leary

A conceptually simple physical problem which produces a numerically difficult fitting problem involves modeling a radioactive decay chain, with unknown decay rates, to explain a single times series of radiation measurements. Solving the system of ODEs to derive an expression for the observed radiation time series yields a linear combination of real exponentials whose rate constants and amplitudes (linear coefficients) must be estimated by nonlinear least squares. Many years ago, Lanczos called this the "separation of exponentials" problem and vividly demonstrated its ill conditioning [C. Lanczos, "Applied Analysis," Prentice Hall (Englewood Cliffs, 1956) pp. 272-280]. A more recent review of the numerical difficulties has been given by Dianne O'Leary [D.P. O'Leary, *Computing in Science and Engineering* **6** (May-June 2004), pp. 66-69]. The presence of measurement errors in the observed data makes the estimation problem practically impossible if there are more than three species (two decays) in the chain. But recent developments in extragalactic astronomy have renewed interest in chains with three decays. Type Ia supernovae have been the object of much government sponsored research because of their promise as "standard candles" for measuring distances to other galaxies. The light curve of such a supernova is given in Figure 1. It is generally believed that the decaying luminosity, beginning a few days after peak brightness, is powered by the radioactive decays

$$\text{Ni-56} \rightarrow \text{Co-56} \rightarrow \text{Fe-56}\,,$$

even though the observed luminosity decay rates do not exactly match the known terrestrial half lives of the nickel and cobalt isotopes. In 1976 evidence was presented by Rust, et. al. [B.W. Rust, M. Leventhal and S.L. McCall, *Nature* **262** (1976), pp. 118-120] which suggested that this mismatch in rates was caused by an acceleration of the nuclear reactions which arises because they occur in the high density interior of a white dwarf star. The evidence, gleaned from 15 light curves, indicated that for any given supernova, both decay rates were increased by the same factor. This means that for each supernova, the ratio of the two observed rates would be the same as the ratio of the terrestrial half

lives, but the acceleration rate would vary from one supernova to another. Thus only 3 (rather than 4) free parameters were required for the sum of two exponentials used to model the decaying part of the light curve. This reduction is almost inconsequential for modeling only the decaying part of the light curve, but it becomes crucial when the model is extended to also accommodate the rise to maximum luminosity.

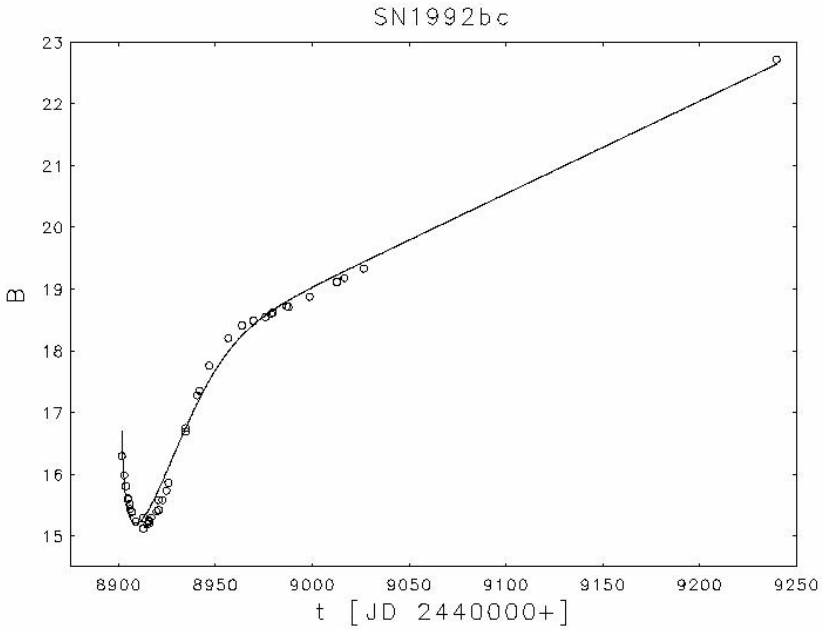

Figure 1. The B-magnitude (blue band) light curve of the Type Ia supernova SN1992bc. The abcissa is time measured in units of Julian Days, and the ordinate is apparent luminosity measured in magnitudes. Because smaller magnitudes indicate greater luminosities, the minimum at approximately 24400008910 days actually corresponds to the peak brightness of the supernova. The circles represent the measured values and the curve is the nonlinear least square fit of the model described in the text below.

A simple model for the entire light curve can be gotten by considering a three stage chain of nuclear reactions of the form

$$\text{(lighter isotopes)} \rightarrow \text{Ni-56} \rightarrow \text{Co-56} \rightarrow \text{Fe-56},$$

with the last two stages being the decays described above. The first stage combines a number of rapidly occurring fusion reactions which build the nickel from lighter nuclei. The model does not consider the details of these reactions, but assumes only that, taken all together, they occur on an exponential time scale with a well defined rate constant to be determined by fitting the measured light curve data. Assuming that all three stages contribute to the total luminosity yields a linear combination of three exponentials with three linear and three nonlinear adjustable parameters. The above-described reduction of the number of effective rate constants from three to two was offset by the inclusion of the time of the initial explosion as an additional free parameter. The six parameter model is completely intractable because of the ill conditioning noted above. But it can be transformed into a model in which, for physical reasons, all six parameters must be nonnegative. This does not alleviate the ill-conditioning, but it suggests the possibility of stabilizing the fits by using a nonnegatively constrained optimization algorithm. The reformulation also isolates the contribution to the luminosity of the first stage of the above reactions, and if that term is dropped from the model, the result is a five parameter model which is not intractable. The curve in Figure 1 is a fit of that reduced

model. Even without the luminosity contribution from the fusion reactions, the fit tracks the data well enough to justify further efforts to stabilize the six parameter fit. The reward for success in such an effort would be considerable because it is well known that the rate of decline in luminosity is correlated with the peak luminosity. Thus, a good fit to the light curve of a distant supernova would yield estimates of both its apparent luminosity, from the light curve itself, and its intrinsic luminosity, from the estimate of the acceleration of the decay rate. The two could then be combined to give an estimate of the distance to the supernova.

Systems Identification and Parameter Estimation

Bert W. Rust

An important scientific modeling problem is to find a system of ordinary differential equations (ODEs) which describe the dynamical relationships between a set of measured time series variables. The ODEs will usually depend on several unknown constants and/or initial values which must be estimated by simultaneously fitting each separate ODE to its corresponding time series of observations. The fitting procedure (e.g., nonlinear least squares) will usually seek to minimize some measure of the mismatch between the solutions to the ODEs and the observations. Designing a measure of the mismatch which properly weights the contribution of each time series may be difficult because the measurements and/or their uncertainties may be numerically incommensurate, and the time series may not all have the same length.

A current example of great interest involves modeling the relationships between global fossil fuel carbon dioxide emissions $P(t)$, atmospheric concentrations of carbon dioxide c(t), and global average tropospheric temperatures $T(t)$. Good measured time series of annual values of these quantities are readily available on the Web. Previous work [B.W. Rust, ICCS 2004, *Lecture Notes in Computer Science* **3039** (2004), pp. 1226-1233] has suggested the following system of ODEs for modeling these three time series,

$$\frac{dP}{dt} = \alpha P - \beta\left\{\eta P + A\cos\left[\frac{2\pi}{\tau}(t+\phi)\right]\right\}P\,, \qquad P(t_0) = P_0$$

$$\frac{dc}{dt} = \gamma P\,, \qquad c(t_0) = c_0$$

$$\frac{dT}{dt} = \eta P + A\cos\left[\frac{2\pi}{\tau}(t+\phi)\right], \qquad T(t_0) = T_0$$

with free parameters α, β, η, A, τ, ϕ, P_0, γ, c_0, and T_0. Evidence for the indicated feedback between $T(t)$ and $P(t)$ was first noted in 1982 [B.W. Rust and B.L. Kirk, *Environment International* **7** (1982), pp. 419-422] and updated in 2003 [B.W. Rust, *Computing in Science and Engineering*, **5** (2003), pp. 74-79]. Evidence for the very simple relation between $c(t)$ and $P(t)$ was given in the ICCS 2004 paper noted above. The connection between $c(t)$ and $T(t)$ is the most uncertain link in the system. The above equations assume a linear relation between the two. Although this is a very simple assumption, it seems to be a good first approximation. It also allows the second equation to be dropped and the first and third to be simultaneously fit to their respective time series with only eight free parameters.

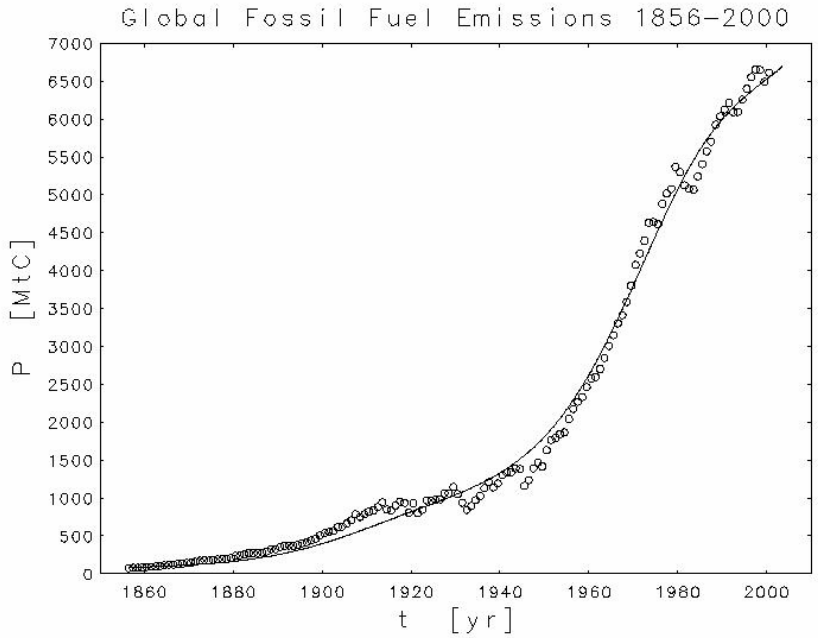

Figure 1. Annual global total fossil fuel carbon dioxide emissions measured in megatons of carbon. The circle are the observed values, and the curve is the *P(t)* fit obtained by simultaneously fitting the first and third ODEs in the above system to their respective data sets.

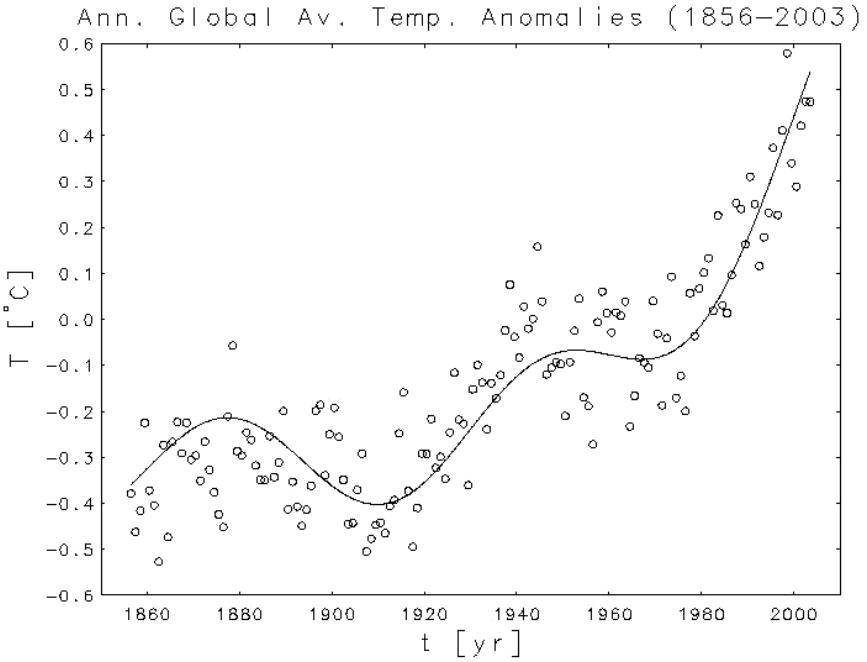

Figure 2. Annual global average tropospheric temperature anomalies (departures from the average temperature for the period 1961-1990) measured in degrees Centigrade. The circles are the observed values, and the curve is the *T(t)* fit obtained by simultaneously fitting the first and third ODEs in the above system to their respective data sets.

Plots of the *P(t)* and *T(t)* time series are given in Figures 1 and 2. The fits were obtained by combining a nonlinear least squares code with an adaptive multi-value ODE integrator. The quantity minimized was a linear combination of the sums of squared residuals for the two separate fits. Inspecting the two plots reveals that the magnitudes of the *P(t)* measurements are roughy 10,000 time larger than those for the temperature measurements, so in the first attempt, the observations in each time series were weighted inversely with the largest magnitude measurement in that series. This produced a good fit for the temperatures but a not so good fit for the emissions. Adding additional weighting for the emissions improved that fit but the temperatures fit was not as good as before. It was easy to improve one fit at the expense of the other by varying the relative weighting. The fits shown here were obtained by weighting the emissions data with an additional factor of 20. That value was a compromise chosen subjectively by inspecting the two fits for several different additional weighting factors. Thus far, no attempt has been made to optimize the choice because other considerations seem more important.

The most important of these considerations is a more realistic relation between *c(t)* and *T(t).* Studies of proxy records obtained from Antarctic ice cores, spanning more than 400,000 years, indicate slight, but not drastic, departures from a linear relation. The small relative uncertainties in the 8 parameter estimates obtained here, and the absence of any large correlations between them, suggest that the data may support at least one more adjustable parameter. The next step will be to replace the linear relation between *c(t)* and *T(t)* with a power law in which the exponent is also a free parameter.

Using a more complex relation between *T(t)* and *c(t)* will require that the *c(t)* time series also be included in the simultaneous fits. This will complicate the choice of weights for the sums of squared residuals because the *c(t)* data go back only to 1959. But the *c(t)* measurements are more precise than those for the other two time series, so the weighting must be adjusted to assure a good fit to them. If such a fit is also accompanied by good fits to the other two data sets, then confidence in the model will be enhanced.

A successful completion of the program outlined above would provide a predictive tool for informing policy decisions on future fossil fuel use. For example, by altering the differential equation for *P(t)* to conform to the provisions of the Kyoto treaty, and comparing the extrapolation of the altered model into the future with the one gotten by continuing on with the current model would allow one to predict whether or not the adoption of the Kyoto treaty would actually produce a significant reduction in the rate of global warming. Replacing the *P(t)* equation with one which provides for a gradual replacement of fossil fuels with alternative energy sources would allow a prediction of the final equilibrium temperature and the time scale on which it would be attained.